THE UNIVERSITY OF

WARWICK

Original citation:
Segercrantz, N., Makkonen, I., Slotte, J., Kujala, J., Veal, T. D., Ashwin, M. J. and Tuomisto, F.. (2015) Increased p-type conductivity in GaNxSb1−x, experimental and theoretical aspects. Journal of Applied Physics, 118 (8). 085708.

Permanent WRAP url:
http://wrap.warwick.ac.uk/74454

Copyright and reuse:
The Warwick Research Archive Portal (WRAP) makes this work by researchers of the University of Warwick available open access under the following conditions. Copyright © and all moral rights to the version of the paper presented here belong to the individual author(s) and/or other copyright owners. To the extent reasonable and practicable the material made available in WRAP has been checked for eligibility before being made available.

Copies of full items can be used for personal research or study, educational, or not-for-profit purposes without prior permission or charge. Provided that the authors, title and full bibliographic details are credited, a hyperlink and/or URL is given for the original metadata page and the content is not changed in any way.

Publisher statement:
Copyright (2015) AIP Publishing. This article may be downloaded for personal use only. Any other use requires prior permission of the author and AIP Publishing.

The following article appeared in Segercrantz, N., Makkonen, I., Slotte, J., Kujala, J., Veal, T. D., Ashwin, M. J. and Tuomisto, F.. (2015) Increased p-type conductivity in GaNxSb1−x, experimental and theoretical aspects. Journal of Applied Physics, 118 (8). 085708 and may be found at http://dx.doi.org/10.1063/1.4929751 .

A note on versions:
The version presented in WRAP is the published version or, version of record, and may be cited as it appears here.For more information, please contact the WRAP Team at: publications@warwick.ac.uk

warwick**publications**wrap

highlight your research

http://wrap.warwick.ac.uk/
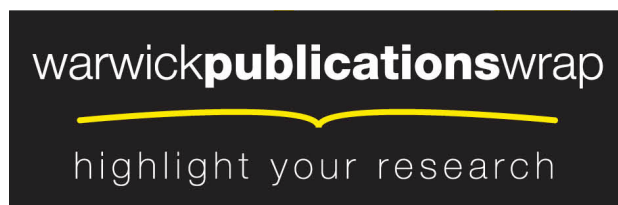
Increased *p*-type conductivity in GaN$_x$Sb$_{1-x}$, experimental and theoretical aspects

N. Segercrantz,[1,a)] I. Makkonen,[1] J. Slotte,[1] J. Kujala,[1] T. D. Veal,[2] M. J. Ashwin,[3] and F. Tuomisto[1]

[1]*Department of Applied Physics, Aalto University, P.O. Box 14100, FIN-00076 Aalto Espoo, Finland*
[2]*Department of Physics and Stephenson Institute for Renewable Energy, University of Liverpool, Liverpool L69 7ZF, United Kingdom*
[3]*Department of Chemistry, University of Warwick, Coventry CV4 7AL, United Kingdom*

The large increase in the *p*-type conductivity observed when nitrogen is added to GaSb has been studied using positron annihilation spectroscopy and *ab initio* calculations. Doppler broadening measurements have been conducted on samples of GaN$_x$Sb$_{1-x}$ layers grown by molecular beam epitaxy, and the results have been compared with calculated first-principle results corresponding to different defect structures. From the calculated data, binding energies for nitrogen-related defects have also been estimated. Based on the results, the increase in residual hole concentration is explained by an increase in the fraction of negative acceptor-type defects in the material. As the band gap decreases with increasing N concentration, the ionization levels of the defects move closer to the valence band. Ga vacancy-type defects are found to act as positron trapping defects in the material, and the ratio of Ga vacancy-type defects to Ga antisites is found to be higher than that of the *p*-type bulk GaSb substrate. Beside Ga vacancies, the calculated results imply that complexes of a Ga vacancy and nitrogen could be present in the material. © 2015 AIP Publishing LLC. [http://dx.doi.org/10.1063/1.4929751]

I. INTRODUCTION

Dilute III–V–nitride semiconductors have recently received more attention due to their potential applications in optoelectronic devices. By substituting the group V-atom with low concentrations of nitrogen, large band gap reductions corresponding to wavelengths in the long or very long–wavelength infrared ranges have been reported.[1–12] The strong modification of the conduction band when dilute amounts of the host anion of the compound semiconductor is replaced is thought to be caused by N-induced states lying near to the conduction band minimum.[13–21]

For the alloy GaN$_x$Sb$_{1-x}$, the band gap red shift is especially large. A 300 meV reduction was reported[1,21–23] when incorporating 1% N into GaSb compared to the significantly smaller band gap reduction of 180 meV/% N for GaN$_x$As$_{1-x}$.[10] The 2–5 μm spectral range of the ternary alloy makes GaN$_x$Sb$_{1-x}$ a suitable candidate for mid-infrared applications. The quaternary alloy Ga$_{1-y}$In$_y$N$_x$Sb$_{1-x}$ can in turn be lattice matched to GaSb having a range of applications such as long wavelength infrared sources.[24] In addition to a large band gap reduction, an increase in the residual hole concentration by two orders of magnitude, from 10^{16} to 10^{18} cm^{-3}, has been reported when N is added to GaSb.[2,9,20,23] The increased acceptor concentration is speculated to be caused by defect states in the material; however, conclusive results on this matter have not been published.

The binary compound gallium antimonide (GaSb) is an interesting material both from a device and from a fundamental point of view (for a review, see Ref. 25). The material can

be used in long wavelength technologies, high-frequency electronic devices, and optoelectronic devices. Undoped GaSb is always *p*-type with the residual hole concentration varying between 10^{16} and 10^{17} cm^{-3} depending on the growth method.[25,26] The cause of the *p*-type conductivity has been studied using positron annihilation spectroscopy.[27–35] Positron annihilation spectroscopy is a non-destructive technique and a powerful method for studying neutral or negative open volume defects in solids.[36] Due to its charge, the positron experiences the absence of a positive nucleus as a potential well. Open-volume defects such as vacancies can therefore trap positrons before annihilation. The reduced fraction of positrons annihilating with core electrons leads to a narrowing of the Doppler broadened 511 keV positron–electron annihilation line compared to that of a defect-free bulk. The reduced electron density at an open-volume defect leads, in turn, to a longer positron lifetime. The positrons can also be localized at hydrogen-like Rydberg states around negative ions. Usually, the binding energy of such states is low enough for the positrons to detrap already at room temperature (RT).

Using positron annihilation lifetime spectroscopy on electron-irradiated Czochralski-grown GaSb, Ling *et al.*,[27] and later Ma *et al.*,[28] characterized two gallium vacancy (V_{Ga})-related defects with different microstructures. In the same reports, an acceptor related to the gallium antisite (Ga$_{Sb}$) was identified from photoluminescence and temperature dependent Hall measurements. This antisite was believed to be responsible for the *p*-type behaviour in GaSb. Kujala *et al.*[35] performed positron lifetime and Doppler broadening measurements on Czochralski-grown undoped GaSb of *p*-type and Te-doped, *n*-type GaSb. The results

a)natalie.segercrantz@aalto.fi

showed that the main defect responsible for the acceptor type behaviour in the bulk GaSb substrates is the Ga_{Sb} and that these antisites compete with the Ga vacancies in trapping positrons well above RT. Using positron annihilation spectroscopy in Doppler broadening mode, molecular beam epitaxy (MBE)-grown GaSb:Bi layers were studied by the group at Aalto University.[34] The results indicated that for the MBE-grown epitaxial layers, the Ga vacancy plays a more significant role in the p-type conductivity and that the residual hole concentration could be caused by different defects in GaSb grown with different methods.

In this paper, we study the cause of the increased p-type conductivity in MBE-grown GaN_xSb_{1-x} epitaxial layers using both positron annihilation measurements and *ab initio* calculations. In order to verify that lattice mismatches do not play a significant role in the positron trapping, epitaxial layers grown on both GaAs and GaSb are studied. In Sec. II, the methods employed in this paper are described along with the sample preparation. In Sec. III A, the experimental data from conventional and coincidence Doppler broadening measurements are analyzed. Calculations of momentum distributions of annihilating electron–positron pairs and binding energies for different defect structures are presented in Sec. III B. The interpretation of the results is discussed in Sec. III C, and in Sec. IV conclusions are presented.

II. METHODS

A. Experiment

Two sets of GaN_xSb_{1-x} samples were grown by plasma assisted MBE. The first set was grown to a thickness of approximately $2\,\mu m$ ($1.5\,\mu m$ for the GaSb film) on semi-insulating GaAs (001) substrates at QinetiQ Ltd., Malvern, with the N content varied by changing the substrate temperature between 360 and $440\,°C$ with the growth rate fixed at $0.8\,\mu m\ h^{-1}$.[2] The N contents of the relaxed films were determined from x-ray diffraction reciprocal space mapping to vary from 0.18% to 1.31%. The films in the second set were grown to thicknesses in the range 0.33 to $0.40\,\mu m$ pseudomorphically on GaSb (001) substrates at the University of Warwick with N contents from x-ray diffraction of 0.56% to 2.32%, varied by altering the growth rate at a fixed growth temperature of $320\,°C$.[11,24] The optical properties of these samples are reported in Ref. 20. The room temperature hole concentrations and mobilities, determined from Hall effect measurements for the epitaxial layers grown on semi-insulating GaAs substrates, are shown in Fig. 1. The GaSb film grown on GaAs has a hole density of $2.6 \times 10^{16}\,cm^{-3}$. The hole density in the GaNSb films on the same substrate is two orders of magnitude higher and increases with increasing N content from $1.6 \times 10^{18}\,cm^{-3}$ to $6.0 \times 10^{18}\,cm^{-3}$. The hole mobility is $730\,cm^2\ V^{-1}\ s^{-1}$ for the GaSb/GaAs film and in the range 100 to $180\,cm^2\ V^{-1}\ s^{-1}$ for the GaNSb/GaAs films with a general trend of decreasing mobility as the hole density increases with N content.

For the conventional Doppler broadening measurements presented in this study, a monoenergetic variable energy $(0.5 - 25\,keV)$ slow positron beam was used. The setup was equipped with a HPGe (high-purity germanium) detector that had an energy resolution of $1.15\,keV$ at $511\,keV$. For
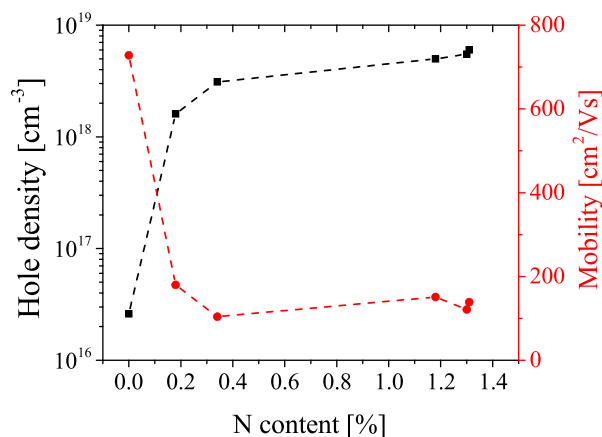

FIG. 1. Hole densities and mobilities from RT Hall measurements plotted against the N content for the GaN_xSb_{1-x} layers on GaAs.

describing the results reported in this article, the conventional line-shape parameters S and W are used.[36,37] The S parameter is defined as the fraction of annihilation events in the central region of the peak thus mainly describing positrons annihilating with low momentum valence electrons. The W parameter is defined in a similar manner as the fraction of annihilation events in the high momentum region. The S parameter window was set to $|p| < 0.4$ a.u. and the W parameter window to 1.6 a.u. $< |p| < 4.0$ a.u.

For materials with more than one positron annihilation state, e.g., materials with an epitaxial layer on a substrate, the line-shape parameters are a superposition of the different annihilation states weighted by the fraction of positrons annihilating at that certain state. By plotting the results in the S–W plane, the different annihilation states can be studied. If, for example, two annihilation states are present in the material, the measured results should lie on a straight line between the characteristic (S, W) values for these two states. The slope of the line and the (S, W) values are characteristic for the specific annihilation state and independent of the positron trapping fraction.

In order to improve the measured peak-to-background ratio and thereby achieve a higher statistical accuracy of the high-momentum region, coincidence Doppler broadening measurements were carried out. For detecting both annihilation photons, a variable energy slow positron beam equipped with a HPGe-detector with resolution $1.24\,keV$ at $511\,keV$ was gated by the signal from another detector. For carrying out the coincidence Doppler measurement at $60\,K$, a sample holder in thermal contact with a closed cycle helium cryostat was used. In order to probe the GaN_xSb_{1-x} epitaxial layers, positron implantation energies of 2.5 and $10\,keV$ were used for the $\sim$350 nm and $\sim$2 μm thick layers, respectively. For achieving statistical reliability, 10^6 and 10^7 annihilation events were collected for each measurement point for the conventional and coincidence measurements, respectively. For more details on the experimental technique, see Ref. 36.

B. Computational

The momentum distributions for electron–positron pairs annihilating in different structures were calculated using

first-principle methods. In order to take into account the interaction between the positron and the electron in the solid, the so-called two-component density functional theory (DFT) was applied.[38] The positron is assumed not to affect the average electron density $n_-(\mathbf{r})$ of the system and the zero-positron density limits ($n_+ \to 0$) of the enhancement and electron–positron correlation energy functionals are used. For electron–electron exchange and correlation, the local-density approximation (LDA) is used. The Kohn-Sham equation of the single positron particle is solved in the potential

$$V_+(\mathbf{r}') = - \int d\mathbf{r}' \frac{n_-(\mathbf{r}')}{|\mathbf{r} - \mathbf{r}'|} - V_{\text{ext}}(\mathbf{r}) + V_{\text{corr}}(\mathbf{r}), \qquad (1)$$

where the first term is the Hartree potential due to the electrons, $V_{\text{ext}}(\mathbf{r})$ is the external potential caused by the nuclei, and $V_{\text{corr}}(\mathbf{r})$ is the local density approximation for the electron–positron correlation potential at the limit $n_+ \to 0$.

The momentum distribution of the annihilating electron–positron pair is calculated using the state-dependent enhancement scheme,[39] in which a constant electron-state-dependent enhancement factor γ_j is used. The momentum density $\rho(\mathbf{p})$ is written as

$$\rho(\mathbf{p}) = \pi r_e^2 c \sum_j \gamma_j \left| \int d\mathbf{r}\, e^{-i\mathbf{p}\cdot\mathbf{r}} \psi_+(\mathbf{r}) \psi_j(\mathbf{r}) \right|^2, \qquad (2)$$

where the summation runs over occupied Kohn–Sham orbitals $\psi_j(\mathbf{r})$ for the electrons, $\psi_+(\mathbf{r})$ is the positron state corresponding to the potential of Eq. (1), r_e is the classical radius of the electron, and c is the speed of light. The state dependent enhancement factor γ_j is the ratio

$$\gamma_j = \frac{\lambda_j^{(\text{BN–LDA})}}{\lambda_j^{\text{IPM}}} \qquad (3)$$

of the annihilation rates λ_j of the Boronski–Neiminen LDA (BN-LDA) and the independent particle model (IPM). The annihilation rates can be calculated by

$$\lambda_j^{(\text{BN–LDA})} = \pi r_e^2 c \int d\mathbf{r}\, n_+(\mathbf{r}) n_-^j(\mathbf{r}) \gamma(n_-(\mathbf{r})), \qquad (4)$$

$$\lambda_j^{(\text{IPM})} = \pi r_e^2 c \int d\mathbf{r}\, n_+(\mathbf{r}) n_j(\mathbf{r}), \qquad (5)$$

where $\gamma(n_-(\mathbf{r}))$ denotes the enhancement factor for a positron in a homogeneous electron gas with density $n_-(\mathbf{r})$.

The positron lifetime is defined as the inverse of the annihilation rate

$$\lambda = \frac{1}{\tau} = \pi r_e^2 c \int d\mathbf{r}\, n_-(\mathbf{r}) n_+(\mathbf{r}) \gamma(n_-(\mathbf{r})) \qquad (6)$$

and can be calculated once the electron and positron densities $n_-(\mathbf{r})$ and $n_+(\mathbf{r})$ are both solved. $\gamma(n_-)$ denotes the enhancement factor[38] in the LDA.

For the practical calculations presented in this work, the plane-wave code VASP[39] employing the projector augmented-wave (PAW) method[40] was used. The PAW implementation used in the momentum–density calculations[41,42] was based on

the VASP code. The positron was treated using the MIKA/Doppler package.[43] All electronic structure calculations were performed using a 216-atom GaSb zincblende supercell. The defect structures were relaxed with a convergence criteria for forces of 0.01 eV/Å also taking into account the forces exerted on the ions by the localized positron. An energy cut-off of 283 eV was used for the binary structures of GaSb, whereas a cut-off of 400 eV was used for structures with nitrogen. For estimating the binding energies of nitrogen atoms to a Ga vacancy, an energy cut-off of 400 eV was used for all structures. Gallium 3d electrons were treated as valence electrons. The Brillouin zone was sampled with a 2^2 Monkhorst–Pack k-point mesh. The calculated spectra were then convoluted with the resolution of the Doppler measurements.

III. RESULTS AND ANALYSIS

A. Doppler broadening measurements on MBE-grown GaN$_x$Sb$_{1-x}$

Figure 2 shows the measured line-shape S parameter as a function of positron implantation energy for the GaN$_x$Sb$_{1-x}$ epitaxial layers grown on GaAs and GaSb, respectively. The mean positron implantation depth is also indicated. As can be seen from the figure, the S parameter decreases with increasing nitrogen content. For the epitaxial layers grown on GaSb, the decrease in S parameter is not as
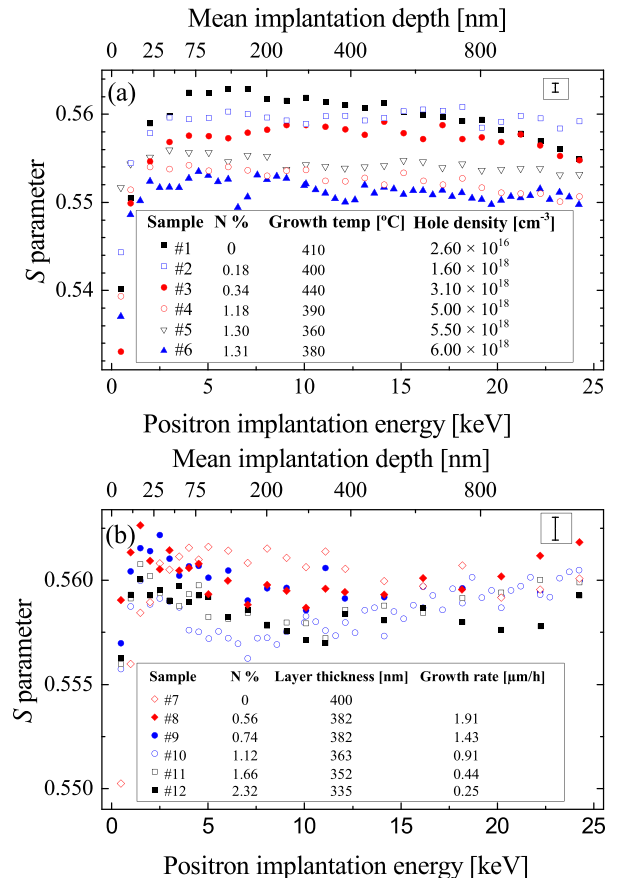

FIG. 2. The S parameters as a function of positron implantation energy for the GaN$_x$Sb$_{1-x}$ epitaxial layers grown on (a) a GaAs and (b) a GaSb substrate. The mean positron implantation depth is indicated. A typical error bar of the data points is shown in the top right corner.

significant as for the layers grown on GaAs; however, it is still visible at energies of 2–7 keV when most of the detected intensity is coming from positrons annihilating in the epitaxial layer. For both the layers grown on GaAs and on GaSb, the highest S parameter of each series corresponds to the sample without nitrogen in the epitaxial layer, namely, samples 1 and 7.

The $W(S)$-plot for the GaN_xSb_{1-x} epitaxial layers grown on GaAs is illustrated in Fig. 3. The measured points shown as larger symbols in the figure correspond to data measured at a positron implantation energy of 10 keV. The positron annihilation surface state is indicated in the figure, and the substrate state of GaAs not shown in the figure was measured as (0.537, 0.034). Due to the thickness of the layers, a considerable fraction of the positrons annihilate in the epitaxial layer even at the highest implantation energies, and the (S, W) value of substrate state is therefore not reached. When moving from the surface state towards the substrate state, the measured (S, W) values of the GaN_xSb_{1-x} layers form a blunt triangle, indicating that the positron trapping into one type of defect is not in saturation but that the measured results are a superposition of the different annihilation states present in the material.[34,44] A similar trend is seen in the measured (S, W) data for the GaN_xSb_{1-x} layers grown on GaSb not shown here. Compared to the sharp turning points in the S–W plane of the results measured for the MBE-grown GaSb:Bi epitaxial layers in Ref. 34, the fraction of positrons trapping into open-volume defects seem to be lower for the GaN_xSb_{1-x} layers.

The coincidence Doppler broadening ratio curves for the GaN_xSb_{1-x} layers measured at RT are illustrated in Fig. 4. Positron implantation energies of 2.5 and 10 keV were used for probing the epitaxial layer grown on GaSb and on GaAs, respectively. For comparison, the ratio curve of the GaSb epitaxial layer grown without a Bi flux measured in Ref. 34 is shown in Fig. 4(b). The measured data have been scaled to the spectrum of p-type Czochralski-grown bulk GaSb substrate measured at RT in Ref. 35. The concentration of V_{Ga}
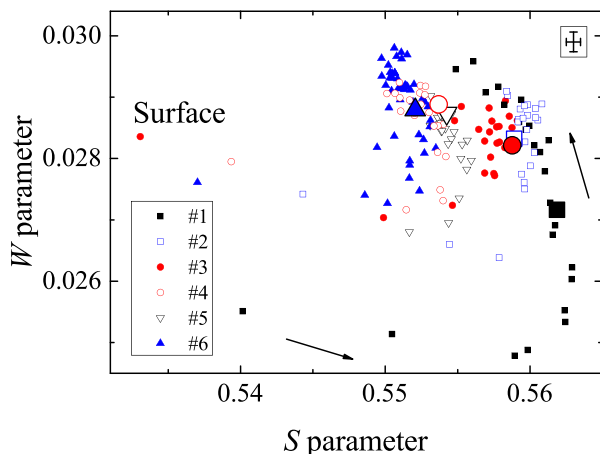

FIG. 4. Ratio curves of the intensity from coincidence Doppler measurements at RT of the GaN_xSb_{1-x} layers grown on (a) a GaAs and (b) a GaSb substrate. A positron implantation energy of 10 keV was used for the layers on GaAs, and 2.5 keV for the layers on GaSb. The windows of the line-shape parameters are sketched. The inset in (a) shows the results from measurements at 60 K and RT for sample 6. The data are scaled to the p-type bulk GaSb substrate.[35] The dashed line indicates the reference.

for the p-type GaSb was estimated to be $3 \times 10^{16}\,cm^{-3}$ and the Ga_{Sb} concentration was $2 \times 10^{17}\,cm^{-3}$.

When illustrating coincidence Doppler broadening data, the results are usually scaled to a defect-free bulk enabling the study of the details of the annihilation line. Since undoped GaSb is p-type with a measurable Ga vacancy and antisite concentration, a conventional defect-free reference is not available for scaling our measured results. However, using the p-type bulk GaSb substrate as in Fig. 4 produces ratio curves with the typical fingerprint of group III vacancies in III–V compounds.[45–49] For comparison, in Fig. 5, the coincidence Doppler broadening results for the GaN_xSb_{1-x} layers on GaAs along with the p-type bulk GaSb substrate have been scaled to sample 6. This sample was chosen due to its intensity at low momenta and corresponding S parameter being lower than that of the p-type bulk GaSb substrate. The structure of the ratio curves in Fig. 5 does not resemble any of the measured group III vacancy ratio curves. Hence, in the following, only the figures of the measured coincidence Doppler broadening results where the p-type bulk GaSb substrate is used as reference will be included in the discussion.

The measured ratio curves of the GaN_xSb_{1-x} layers shown in Fig. 4 clearly differ from the p-type bulk GaSb substrate used as a reference. The structures of the curves have a

FIG. 3. $W(S)$ plot for the GaN_xSb_{1-x} epitaxial layers grown on a GaAs substrate. The arrows indicate increasing positron implantation energy. The surface annihilation state is indicated in the figure, and the larger symbols correspond to data measured at an implantation energy of 10 keV. The substrate state of GaAs not shown in the figure was measured as (0.537, 0.034). Typical error bars of the data points are shown in the top right corner.
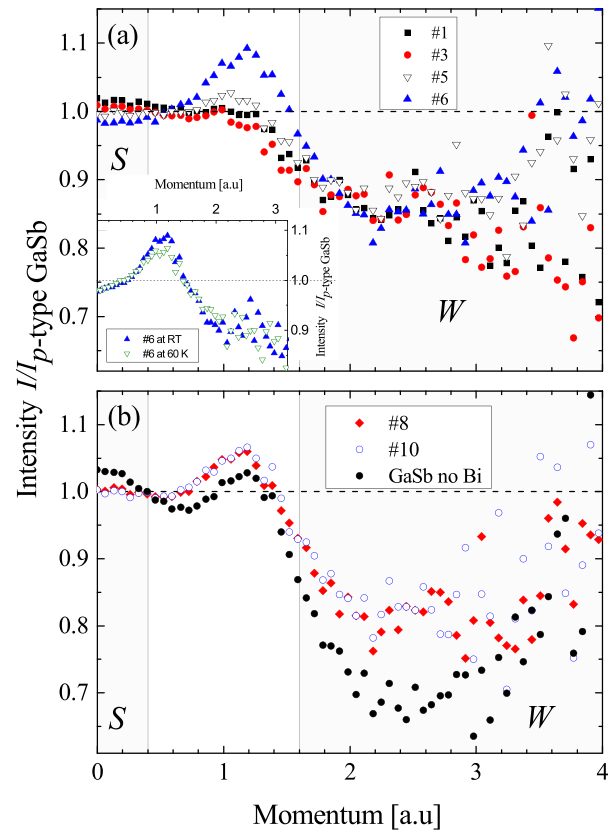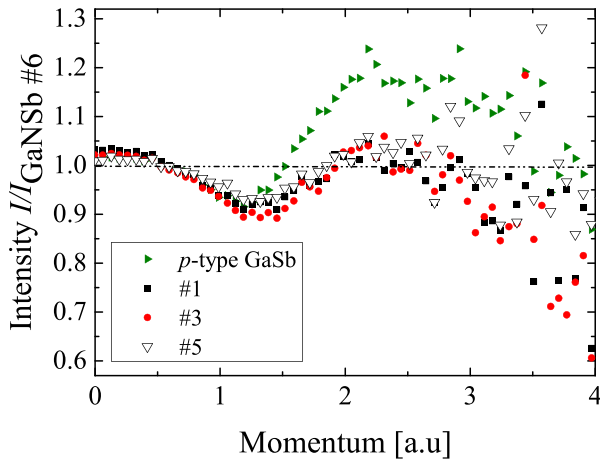
FIG. 5. Ratio curves of the intensity from coincidence Doppler measurements at RT of GaN$_x$Sb$_{1-x}$ layers grown on GaAs and of the *p*-type bulk GaSb substrate. The data are scaled to the GaN$_x$Sb$_{1-x}$ sample 6. The dashed line indicates the reference.

similar appearance as the ratio curves for the GaSb:Bi layers measured in Ref. 34, indicating that Ga vacancy-type defects are present in this material as well. Also, the ratio of the Ga vacancy-type defects to the Ga antisite defect concentration seems to be higher than that of the *p*-type bulk GaSb substrate. Compared to the GaSb epitaxial layer grown without a Bi flux shown in Fig. 4(b), the ratio curve of sample 1 without N has less structure. The lower intensity at low momenta and the smaller intensity dip at $p > 2$ a.u. indicates a decreased positron trapping into open-volume defects, as did the $W(S)$ plot results shown in Fig. 3. This is probably due to the different growth conditions of the two samples. For the samples with nitrogen in the epitaxial layer, an increase in intensity in the peak at ∼1.2 a.u. and a decrease in intensity at low momenta corresponding to the decrease in the S parameter can be seen when nitrogen is added. For both samples 5 and 6, the intensity at low momenta drops below that of the reference.

A coincidence Doppler broadening measurement at 60 K was performed for the sample showing the most structure in Fig. 4(a), namely, sample 6 with the highest N content of the layers grown on GaAs. The same positron implantation energy of 10 keV was used for this measurement. The result along with a RT measurement is illustrated in the inset of Fig. 4(a). The change in temperature appears to have a very modest effect on the ratio curve. The intensity at low momenta slightly increases as the peak at ∼1.2 a.u. decreases. The similar appearance of the ratio curves measured at RT and 60 K for the GaN$_x$Sb$_{1-x}$ layers indicates that the positron annihilation states in the material are the same for both measurements. The Ga vacancy-type defects seem to be able to compete in trapping positrons with the Ga antisites even at low temperatures.

B. Theoretical calculations

Momentum-distribution calculations of different open-volume structures and of nitrogen-related defects were performed within the DFT framework. The calculated open-volume structures consisted of a Ga vacancy–Ga

antisite complex ($V_{Ga} - Ga_{Sb}$), a divacancy ($V_{Ga} - V_{Sb}$), and complexes consisting of a Ga vacancy and one, two, or four nitrogen atoms on the neighbouring antimony lattice sites ($V_{Ga} - N_{Sb}$, $V_{Ga} - 2N_{Sb}$, and $V_{Ga} - 4N_{Sb}$). The results are illustrated in Fig. 6 along with the calculated ratio curves of the V_{Ga} and the V_{Sb} performed in Ref. 34. The data are scaled to the calculated defect-free GaSb lattice. The insets in Figs. 6(a) and 6(b) show the calculated positron lifetimes (τ) in the structures. Generally, for comparison with experimental data, the difference $\tau_{bulk} - \tau_{defect}$ gives a reliable value rather than the absolute values.[50]

According to recent DFT calculations,[17,51] the $N_{Sb} - N_{Sb}$ pair is one of the most favourable configurations for N in GaN$_x$Sb$_{1-x}$ along with the N_{Sb}. Some experimental studies have also speculated on the $N_{Sb} - N_{Sb}$ pair formation and in its possible bound states in the band gap.[20,52] Structures consisting of an isolated nitrogen atom (N_{Sb}) and two nitrogen atoms on next-nearest-neighbour antimony lattice sites ($N_{Sb} - N_{Sb}$) were therefore calculated. However, according to our calculations, these structures are not able to trap positrons.

From our calculated results, a larger open volume of the defect corresponds to a higher τ value. This is to be expected since the positron lifetime is inversely proportional to the electron density encountered by the positron.[36] By replacing a large atom like Sb in GaSb with N, a much smaller atom, the open volume around the lattice site is increased. Our calculations also show that the N atom relaxes outwards from the Sb lattice site leading to an even larger open volume
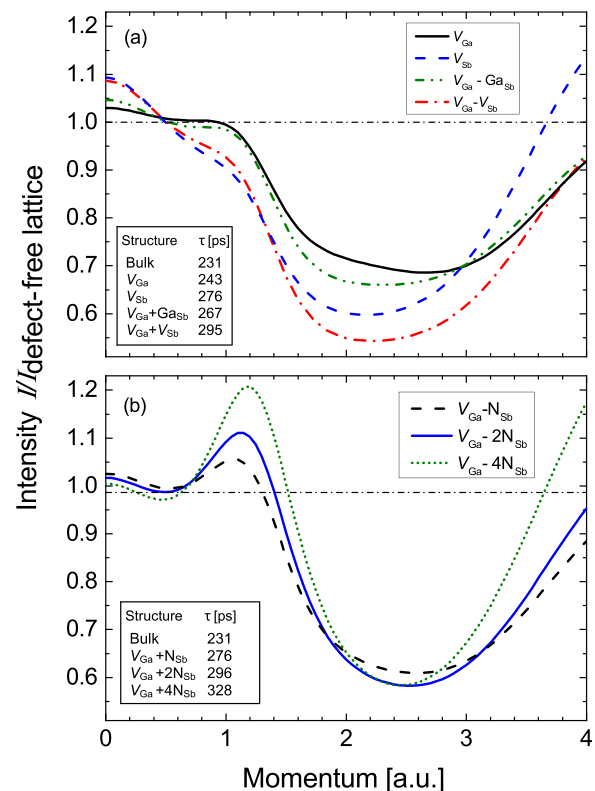

FIG. 6. Ratio curves of calculated Doppler spectra for open-volume (a) intrinsic defects and (b) N-related defects. The calculated τ in the different structures is indicated in the tables. The dashed line indicates the defect-free lattice used as a reference.

around the V_{Ga}. This is in line with previous computational studies[17] showing that the Ga–N bond is much shorter than the Ga–Sb bond. Compared to the V_{Ga}, the $V_{Ga} - 4N_{Sb}$ complex, e.g., has therefore a larger open volume and a 83 ps higher τ. A similar increase in the intensity at low momenta ($p < 0.4$ a.u.) corresponding to the S parameter is not observed. Instead, the intensity at low momenta decreases, while the τ and the open volume of the defect increase with increasing number of neighbouring N atoms to the Ga vacancy. The conventional interpretation of the S parameter as an indicator of open-volume is thus not necessarily correct for strongly cation–anion-mismatched compounds such as GaNSb studied here, an observation already made in the case of InN.[47]

Results obtained with the atomic superposition (ATSUP) method[53] for the calculated structures give information on the contributions of different electronic shells and their relative intensities in the Doppler broadening spectrum. The systematic trend in the ratio curves for the Ga vacancy–nitrogen complexes compared to the Ga vacancy visible in Fig. 6(b) can be explained based on these results (not shown here). As the number of N per V_{Ga} is increased, the number of neighbouring Sb atoms is in turn reduced. The decrease in the intensity at low momenta is due to the reduced positron annihilation with Sb $5p$ valence electrons. The peak seen at 1.2 a.u. is most pronounced for the $V_{Ga} - 4N_{Sb}$ complex and is caused by an increased fraction of positrons annihilating with N $2p$ electrons. The reduced overlap between the positron wavefunction and that of the Sb $4d$ and Ga $3d$ electrons leads to the intensity dip at higher momenta ($p > 2$ a.u.).

Using the calculated total energies for structures in GaSb and GaN$_x$Sb$_{1-x}$, the relative binding energies for neutral Ga vacancy–nitrogen complexes could be estimated. However, binding energies for the corresponding charged defects could not be reliably estimated since the LDA used for the electron–electron exchange and correlation in our calculations substantially underestimates the band gap. The binding energy of n number of nitrogen atoms decorating a Ga vacancy relative to the case of a Ga vacancy and n number of structures consisting of a N antisite can be written as

$$E_b = E[V_{Ga} - nN_{Sb}] + nE[\text{bulk}] - nE[N_{Sb}] - E[V_{Ga}], \quad (7)$$

where each term $E[\text{structure}]$ is the total energy calculated for that specific structure. For one N atom neighboring the Ga vacancy, the relative binding energy was estimated to be -0.21 eV, whereas the binding energy of two N atoms was -0.60 eV, and therefore the binding energy for a second N atom bound to the $V_{Ga} - N_{Sb}$ complex was -0.39 eV. Here, the negative sign on the binding energy indicates that the total energy of the system is reduced and therefore that the nitrogen atoms are bound to the vacancy. The estimated binding energies for the complexes serve as an indicator that nitrogen bound to a Ga vacancy might be the more favorable configuration compared to neutral isolated Ga vacancies and N antisites in GaN$_x$Sb$_{1-x}$.

Comparing the calculated spectra with the experimental ones, the signal of the Sb vacancy-related defects shown in Fig. 6(a) is found to be very different from the measured

results in Fig. 4. For the ratio curves of the V_{Sb} and the $V_{Ga} - V_{Sb}$, the rather high intensity at low momenta along with the low intensity in the vicinity of 1.2 a.u. rule these defects out as possible positron trapping defects in the studied layers. It is to be noted that the structure of these Sb-related ratio curves are not in agreement with the measured ratio curves scaled to the GaN$_x$Sb$_{1-x}$ layer illustrated in Fig. 5. This provides additional confirmation of our choice of reference.

The calculated results for the Ga-vacancy related defects are in much better agreement with the experimental results. This is in line with the positron annihilation spectroscopy results for both bulk and epitaxial GaSb[34,35] as well as with the interpretations presented above for the experimental data. The structure of the ratio curves consisting of the Ga vacancy-nitrogen complexes seems to be somewhat similar to the measured results for the epitaxial layers with nitrogen. The measured decrease in the intensity at low momenta and increase in the peak intensity at ∼1.2 a.u. with increasing N content agrees rather well with the calculated results for the complexes.

As stressed earlier, the reference of the measured results is not defect-free, whereas the calculated spectra are scaled to a defect-free lattice. In the p-type bulk GaSb substrate, both Ga vacancies and antisites act as positron traps.[35] The comparison between experimental data and calculated results should therefore be done while keeping this in mind. Also, since the measured results indicate that the positron trapping into one type of defect is not in saturation, the measured ratio curves correspond to superpositions of the different annihilation states in the epitaxial layers, whereas the calculated ratio curves correspond to those of single defect states.

C. Discussion

For the studied GaN$_x$Sb$_{1-x}$ layers, a decrease in the line-shape S parameter and corresponding drop in the intensity at low momenta was measured with increasing N content for both epitaxial layers grown on GaAs and on GaSb. From the measured positron data, we conclude that similar types of positron trapping defects exist in both sets of samples; therefore, lattice mismatches do not play a significant role in neither the positron trapping nor in the increased p-type conductivity. Traditionally, a decrease in the S parameter has been interpreted as a reduction in the fraction of positrons trapping into open-volume defects. However, a change in the charge state of the defect can lead to a somewhat different S parameter since the atoms neighboring negative vacancies can relax inwards.[54] For the layers with N, the measured large increase in the p-type conductivity indicates an increase in negatively charged defects in the material. In addition to the increase in charged defects, the calculations indicate that the added nitrogen can also affect the shape of the annihilation line in the case of positrons localizing at or near to nitrogen atoms. Therefore, the conventional interpretation of the line-shape parameters might in this case not be suitable for the studied material.

From the coincidence Doppler broadening results of the GaN$_x$Sb$_{1-x}$ layer measured at RT and 60 K, the decrease in

temperature was concluded to have a very modest effect on the measured Doppler broadening ratio curve. As the temperature decreases, the charged states of the defects become less populated and the concentration of negative acceptor-type defects decreases.[23] The bulk study of GaSb suggests that the $Ga_{Sb}-1/0$ ionization level is closer to the valence band edge than the corresponding level for the Ga vacancy.[35] A larger fraction of the Ga antisites are therefore expected to be negative compared to the Ga vacancies. For both negative ions and negative vacancies, the trapping coefficients at RT are of magnitude $(10^{15} - 10^{16})$ s^{-1} and increase when the temperature decreases. The trapping coefficient of neutral vacancies is temperature-independent and of magnitude $(10^{14} - 10^{15})$ s^{-1}.[37] The similar appearance of the ratio curves measured at RT and 60 K for the GaN_xSb_{1-x} layers indicate that measured signal corresponds to the same positron annihilation states at both temperatures. Therefore, the fraction of negative Ga vacancy-type defects seems to be large enough in order to effectively compete in trapping positrons with the negative antisites even at low temperatures.

Based on the above data of both measured and calculated results for the GaN_xSb_{1-x} layers, the following explanation is proposed: the measured increase in the *p*-type conductivity with increased N content for the GaN_xSb_{1-x} layers is related to a larger fraction of the acceptor-type defects in the material becoming negatively charged. This in turn is due the ionization levels of these defects being pinned to the conduction band edge. When nitrogen is added, the conduction band edge along with the ionization levels shift closer the valence band. Due to the high concentration of the acceptor-type defects, the Fermi level position in the band gap is largely defined by these defects and is expected to lie close to the $-1/0$ ionization levels of the acceptor-type defects. A slight change in this distance between the Fermi level and the ionization levels has, due to the steepness of the Fermi–Dirac distribution, a large impact on the fraction of negativity charged defects. Therefore, as the ionization levels shift closer to the valence band, a larger fraction of the acceptor-type defects becomes negatively charged and the *p*-type conductivity increases. Figure 7 schematically illustrates the band shift using the calculated results[17] for the ionization levels of GaSb as well as the measured bulk results,[35] suggesting that the $-1/0$ level of the Ga vacancy is higher than that of the Ga antisite.

The increase in the N content and in the fraction of negative defects is seen in our positron annihilation spectroscopy measurements as the somewhat differing Doppler broadening ratio curves for the GaN_xSb_{1-x} layers. The similar appearance of the measured ratio curves to that of the GaSb:Bi layers presented in Ref. 34 indicates that positron trapping Ga vacancy-type defects are present in GaN_xSb_{1-x} layers as well. Compared to the *p*-type bulk GaSb substrate, the ratio of the Ga vacancy-type defect concentration to the Ga antisite concentration is higher for the GaN_xSb_{1-x} layers. As seen from the measurement at 60 K, the concentration of the Ga vacancy-type defects is high enough for a large fraction of the defects to be negative at low temperatures and
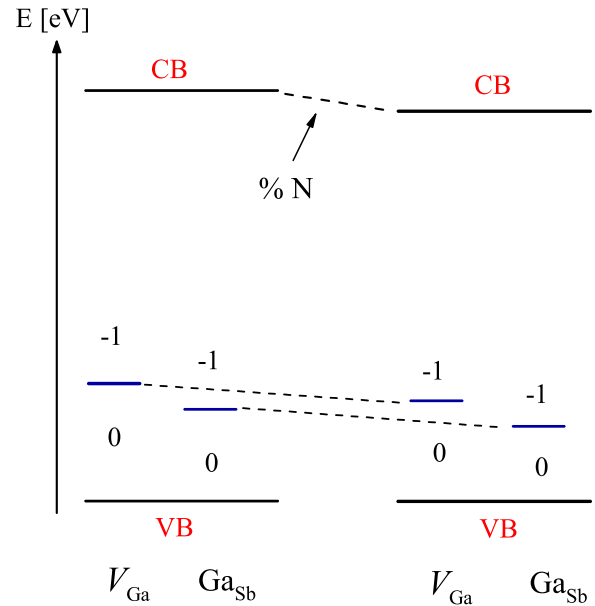

FIG. 7. Schematic illustration of N-induced changes in the ionization levels of acceptor-type defects and the conduction band (CB) edge of GaSb. Only the $-1/0$ level for the acceptor-type defects nearest to the valence band (VB) edge is shown.

effectively compete in trapping positrons with negative Ga antisites.

Beside the V_{Ga} and Ga_{Sb} defects acting as positron traps, the first-principle calculations presented in this study suggest that open-volume defect complexes consisting of a V_{Ga} and nitrogen on the antimony lattice site could also be present in the material. The calculated negative binding energies indicate that the neutral Ga vacancy–nitrogen complexes being energetically more favourable structures compared to, e.g., the neutral Ga vacancy. The systematic trend of a decrease in the intensity at low momenta and increase in the intensity peak at 1.2 a.u. visible in the calculated spectra when adding neighbouring N atoms to the V_{Ga} is also in line with experimental data. However, the change in the fraction of negative Ga vacancy and antisite defects could also have a similar effect on the ratio curves. Also, the binding energies of negative Ga vacancy–nitrogen complexes compared to that of the negative Ga vacancy were not estimated. The $-1/0$ ionization level position of the Ga vacancy–nitrogen complexes to that of the Ga vacancy will ultimately determine the effect of these complexes on the *p*-type conductivity and on the positron annihilation signal. Positron lifetime measurements using a pulsed positron lifetime beam could possibly shed some more light on the concentration of different Ga-vacancy type defects in the GaN_xSb_{1-x} layers.

In order to explain the increased *p*-type conductivity and the results measured in this study, the concentrations of both the negative Ga antisites and the negative Ga vacancy-type defects have to increase with increasing N content. Assuming only a large increase in the concentration of negative open-volume defects (like Ga vacancy-nitrogen complexes and/or Ga vacancies) is not sufficient to explain the experimental data. If the concentration of the negative open-volume defects would be that of the total residual hole concentration measured to a magnitude of 10^{18} cm^{-3}, the total

concentration of neutral and negative defects should be even higher. This high concentration of open-volume defects should compete very effectively in trapping positrons with Ga antisites of the concentration 10^{16}cm^{-3}. The measured signal should therefore correspond to saturation trapping of positrons into these open-volume defects.[36] Since the measured results for the layers indicated that the positron trapping into open-volume defects is not in saturation, and this line of thought can be dismissed.

IV. CONCLUSIONS

In conclusion, MBE-grown GaN_xSb_{1-x} layers on GaSb and on GaAs substrates have been studied using positron annihilation spectroscopy in Doppler broadening mode. Using first-principle methods, momentum distributions of annihilating electron–positron pairs for different defect structures in GaSb and GaN_xSb_{1-x} have been performed and binding energies of neutral nitrogen-related complexes have been estimated. Based on the results, the increase in the *p*-type conductivity for the GaN_xSb_{1-x} layers is explained by an increase in the fraction of negative acceptor-type defects. As the band gap decreases with increasing N content, the ionization levels of the acceptor-type defects move closer to the valence band. Ga vacancy-type defects are concluded to be present in these layers and the concentration of these open-volume defects compared to that of the Ga antisites to be higher than in the bulk *p*-type GaSb substrate. Beside Ga vacancies and Ga antisites acting as positron traps, the first-principle calculations suggest that open-volume defect complexes consisting of a gallium vacancy and nitrogen on the antimony lattice site could also be present in the material.

ACKNOWLEDGMENTS

[1]T. D. Veal, L. F. J. Piper, S. Jollands, B. R. Bennett, P. H. Jefferson, P. A. Thomas, C. F. McConville, B. N. Murdin, L. Buckle, G. W. Smith *et al.*, Appl. Phys. Lett. **87**, 132101 (2005).
[2]L. Buckle, B. R. Bennett, S. Jollands, T. D. Veal, N. R. Wilson, B. N. Murdin, C. F. McConville, and T. Ashley, J. Cryst. Growth **278**, 188 (2005).
[3]M. Weyers, M. Sato, and H. Ando, Jpn. J. Appl. Phys., Part 2 **31**, L853 (1992).
[4]H. P. Xin and C. W. Tu, Appl. Phys. Lett. **72**, 2442 (1998).
[5]G. Pozina, I. Ivanov, B. Monemar, J. V. Thordson, and T. G. Andersson, J. Appl. Phys. **84**, 3830 (1998).
[6]W. G. Bi and C. W. Tu, Appl. Phys. Lett. **69**, 3710 (1996).
[7]T. D. Veal, L. F. J. Piper, P. H. Jefferson, I. Mahboob, C. F. McConville, M. Merrick, T. J. C. Hosea, B. N. Murdin, and M. Hopkinson, Appl. Phys. Lett. **87**, 182114 (2005).
[8]H. Naoi, Y. Naoi, and S. Sakai, Solid-State Electron. **41**, 319 (1997).
[9]L. Buckle, S. D. Coomber, T. Ashley, P. H. Jefferson, D. Walker, T. D. Veal, C. F. McConville, and P. A. Thomas, Microelectron. J. **40**, 399 (2009).
[10]K. Uesugi, N. Morooka, and I. Suemune, Appl. Phys. Lett. **74**, 1254 (1999).
[11]M. J. Ashwin, T. D. Veal, J. J. Bomphrey, I. R. Dunn, D. Walker, P. A. Thomas, and T. S. Jones, AIP Adv. **1**, 032159 (2011).
[12]A. Mondal, T. D. Das, N. Halder, S. Dhar, and J. Kumar, J. Cryst. Growth **297**, 4 (2006).
[13]W. Shan, W. Walukiewicz, J. W. Ager III, E. E. Haller, J. F. Geisz, D. J. Friedman, J. M. Olson, and S. R. Kurtz, Phys. Rev. Lett. **82**, 1221 (1999).
[14]B. N. Murdin, M. Kamal-Saadi, A. Lindsay, E. P. O'Reilly, A. R. Adams, G. J. Nott, J. G. Crowder, C. R. Pidgeon, I. V. Bradley, J.-P. R. Wells *et al.*, Appl. Phys. Lett. **78**, 1568 (2001).
[15]J. Wu, W. Shan, and W. Walukiewicz, Semicond. Sci. Technol. **17**, 860 (2002).
[16]J. D. Perkins, A. Mascarenhas, Y. Zhang, J. F. Geisz, D. J. Friedman, J. M. Olson, and S. R. Kurtz, Phys. Rev. Lett. **82**, 3312 (1999).
[17]V. Virkkala, V. Havu, F. Tuomisto, and M. J. Puska, Phys. Rev. B **85**, 085134 (2012).
[18]E. P. O'Reilly, A. Lindsay, P. J. Klar, A. Polimeni, and M. Capizzi, Semicond. Sci. Technol. **24**, 033001 (2009).
[19]A. Lindsay, E. P. O'Reilly, A. D. Andreev, and T. Ashley, Phys. Rev. B **77**, 165205 (2008).
[20]J. J. Mudd, N. J. Kybert, W. M. Linhart, L. Buckle, T. Ashley, P. D. C. King, T. S. Jones, M. J. Ashwin, and T. D. Veal, Appl. Phys. Lett. **103**, 042110 (2013).
[21]P. H. Jefferson, T. D. Veal, L. F. J. Piper, B. R. Bennett, C. F. McConville, B. N. Murdin, L. Buckle, G. W. Smith, and T. Ashley, Appl. Phys. Lett. **89**, 111921 (2006).
[22]A. Belabbes, M. Ferhat, and A. Zaoui, Appl. Phys. Lett. **88**, 152109 (2006).
[23]D. Wang, S. P. Svensson, L. Shterengas, G. Belenky, C. S. Kim, I. Vurgaftman, and J. R. Meyer, J. Appl. Phys. **105**, 014904 (2009).
[24]M. J. Ashwin, D. Walker, P. A. Thomas, T. S. Jones, and T. D. Veal, J. Appl. Phys. **113**, 033502 (2013).
[25]P. S. Dutta, H. L. Bhat, and V. Kumar, J. Appl. Phys. **81**, 5821 (1997).
[26]F. J. Reid, R. D. Baxter, and S. E. Miller, J. Electrochem. Soc. **113**, 713 (1966).
[27]C. C. Ling, M. K. Lui, S. K. Ma, X. D. Chen, S. Fung, and C. D. Beling, Appl. Phys. Lett. **85**, 384 (2004).
[28]S. K. Ma, M. K. Lui, C. C. Ling, S. Fung, C. D. Beling, K. F. Li, K. W. Cheah, M. Gong, H. S. Hang, and H. M. Weng, J. Phys.: Condens. Matter **16**, 6205 (2004).
[29]S. Dannefaer, W. Puff, and D. Kerr, Phys. Rev. B **55**, 2182 (1997).
[30]J. Mahony, G. Tessaro, P. Mascher, H. Siethoff, and H.-G. Brion, Mater. Sci. Forum **196**, 1449–1454 (1995).
[31]J. Kujala, J. Slotte, and F. Tuomisto, J. Phys.: Conf. Ser. **443**, 012042 (2013).
[32]C. C. Ling, W. K. Mui, C. H. Lam, C. D. Beling, S. Fung, M. K. Lui, K. W. Cheah, K. F. Li, Y. W. Zhao, and M. Gong, Appl. Phys. Lett. **80**, 3934 (2002).
[33]C. C. Ling, S. Fung, C. D. Beling, and W. Huimin, Phys. Rev. B **64**, 075201 (2001).
[34]N. Segercrantz, J. Slotte, I. Makkonen, J. Kujala, F. Tuomisto, Y. Song, and S. Wang, Appl. Phys. Lett. **105**, 082113 (2014).
[35]J. Kujala, N. Segercrantz, F. Tuomisto, and J. Slotte, J. Appl. Phys. **116**, 143508 (2014).
[36]F. Tuomisto and I. Makkonen, Rev. Mod. Phys. **85**, 1583 (2013).
[37]K. Saarinen, P. Hautojärvi, and C. Corbel, Semicond. Semimetals **51**, 209 (1998).
[38]E. Boroński and R. M. Nieminen, Phys. Rev. B **34**, 3820 (1986).
[39]M. Alatalo, B. Barbiellini, M. Hakala, H. Kauppinen, T. Korhonen, M. J. Puska, K. Saarinen, P. Hautojärvi, and R. M. Nieminen, Phys. Rev. B **54**, 2397 (1996).
[40]P. E. Blöchl, Phys. Rev. B **50**, 17953 (1994).
[41]I. Makkonen, M. Hakala, and M. J. Puska, J. Phys. Chem. Solids **66**, 1128 (2005).
[42]I. Makkonen, M. Hakala, and M. J. Puska, Phys. Rev. B **73**, 035103 (2006).
[43]T. Torsti, T. Eirola, J. Enkovaara, T. Hakala, P. Havu, V. Havu, T. Höynälänmaa, J. Ignatius, M. Lyly, I. Makkonen *et al.*, Phys. Status Solidi B **243**, 1016 (2006).
[44]S.-L. Sihto, J. Slotte, J. Lento, K. Saarinen, E. V. Monakhov, A. Y. Kuznetsov, and B. G. Svensson, Phys. Rev. B **68**, 115307 (2003).
[45]S. Hautakangas, I. Makkonen, V. Ranki, M. J. Puska, K. Saarinen, X. Xu, and D. C. Look, Phys. Rev. B **73**, 193301 (2006).
[46]T. Laine, K. Saarinen, J. Mäkinen, P. Hautojärvi, C. Corbel, L. N. Pfeiffer, and P. H. Citrin, Phys. Rev. B **54**, R11050 (1996); I. Makkonen and M. J. Puska, *ibid.* **76**, 054119 (2007).
[47]C. Rauch, I. Makkonen, and F. Tuomisto, Phys. Rev. B **84**, 125201 (2011).

[48]J.-M. Mäki, I. Makkonen, F. Tuomisto, A. Karjalainen, S. Suihkonen, J. Räisänen, T. Y. Chemekova, and Y. N. Makarov, Phys. Rev. B **84**, 081204 (2011).

[49]M. Alatalo, H. Kauppinen, K. Saarinen, M. J. Puska, J. Mäkinen, P. Hautojärvi, and R. M. Nieminen, Phys. Rev. B **51**, 4176 (1995).

[50]K. G. Lynn, J. R. MacDonald, R. A. Boie, L. C. Feldman, J. D. Gabbe, M. F. Robbins, E. Bonderup, and J. Golovchenko, Phys. Rev. Lett. **38**, 241 (1977).

[51]J. Buckeridge, D. O. Scanlon, T. D. Veal, M. J. Ashwin, A. Walsh, and C. R. A. Catlow, Phys. Rev. B **89**, 014107 (2014).

[52]S. Iyer, L. Wu, J. Li, S. Potoczny, K. Matney, and P. R. C. Kent, J. Appl. Phys. **101**, 113508 (2007).

[53]M. J. Puska and R. M. Nieminen, J. Phys. F: Met. Phys. **13**, 333 (1983).

[54]K. Kuitunen, F. Tuomisto, and J. Slotte, Phys. Rev. B **76**, 233202 (2007).